Engineering Conferences International
ECI Digital Archives

10th International Conference on Circulating Fluidized Beds and Fluidization Technology - CFB-10

Refereed Proceedings

Spring 5-2-2011

Fluidized Bed Membrane Reactor for Steam Reforming of Higher Hydrocarbons: Model Sensitivity

M.A. Rakib
University of British Columbia, rakibche@gmail.com

John R. Grace
University of British Columbia, jgrace@chml.ubc.ca

C. Jim Lim
The University of British Columbia, cjlim@chml.ubc.ca

FLUIDIZED BED MEMBRANE REACTOR FOR STEAM REFORMING OF HIGHER HYDROCARBONS: MODEL SENSITIVITY

M.A. Rakib*, J.R. Grace and C.J. Lim
University of British Columbia, Vancouver, Canada V6T 1Z3
* Corresponding author (rakibche@gmail.com),
currently with SABIC T&I, Riyadh 11551, Saudi Arabia

ABSTRACT

A fluidized bed membrane reactor (FBMR) was built and operated at temperatures <600°C to reform higher hydrocarbons like propane and heptane. A two-phase reactor model is utilized to simulate the FBMR with hydrogen withdrawn from both phases. The superficial gas velocities in the reactor change because of variations in molar flow due to reaction and hydrogen withdrawal through the membranes, as well as variations in temperature, pressure and cross-sectional area. Sensitivity studies show that the FBMR performance is primarily controlled by chemical equilibrium and hydrogen permeation through the membranes, while being insensitive to errors in accurately characterizing the chemical kinetics and hydrodynamics.

INTRODUCTION

The increasing demand for hydrogen as an industrial commodity and future energy carrier has intensified research on alternative methods of hydrogen production. Steam reforming is the favoured process for making hydrogen (1). Natural gas is the most widely used feedstock due to its widespread availability. Liquid hydrocarbon feedstocks like naphtha and LPG can be used when natural gas is not available. Higher hydrocarbons like LPG, naphtha, kerosene and diesel are preferable for making hydrogen in mobile applications. In addition, feedstock flexibility is desirable for refineries, which often have seasonal surpluses of some of these hydrocarbons.

The main reactions for steam reforming of higher hydrocarbons are (1):

$C_nH_m + nH_2O \leftrightarrows nCO + (n + m/2)H_2$ $\quad \Delta H°_{298} = 499$ kJ/mol (for n = 3) (1)

$CH_4 + H_2O \leftrightarrows CO + 3\,H_2$ $\quad \Delta H°_{298} = 206$ kJ/mol (2)

$CO + H_2O \leftrightarrows CO_2 + H_2$ $\quad \Delta H°_{298} = -41$ kJ/mol (3)

$CH_4 + 2H_2O \leftrightarrows CO_2 + 4H_2$ $\quad \Delta H°_{298} = 165$ kJ/mol (4)

The yield of hydrogen is limited by the reversibility of reactions (2)-(4). In general, reaction (1) is irreversible for higher hydrocarbons, but methane appears in the reaction mixture due to the reversibility of reactions (2) and (4). In traditional steam reformers, this is overcome by operating at high temperatures. However, elevated temperatures lead to limited pressure ratings of the containment material, catalyst sintering, and high steam-to carbon ratios to minimize catalyst deactivation.

A fluidized bed membrane reactor (FBMR) for steam reforming of natural gas is a potential low-temperature alternative to achieve high hydrogen yields by continuous shifting of equilibrium in the forward direction (2-4). An FBMR has been shown to be flexible; able to process different alkane hydrocarbons (C_nH_m) as the feedstock (5,6), leading to complete conversion of the hydrocarbons to produce maximum hydrogen:

$C_nH_m + 2nH_2O \rightarrow nCO_2 + (2n + m/2)H_2$ (5)

EXPERIMENTAL SETUP

Steam reforming was conducted in a pressure vessel designed to withstand 10 bars gauge at a maximum temperature of 621°C. The dense catalyst bed is contained in a rectangular channel, 1.88 x 10^{-3} m^2 and height of 1.87 m, with an extended circular cross-section, 4.26 x 10^{-3} m^2, above this. Figure 1 portrays the FBMR pressure vessel. Vertical membrane panels (231.8 mm x 73.0 mm x 6.4 mm), with 25 μm thick $Pd_{77}Ag_{23}$ membrane foils bonded on either side, divide the rectangular channel into two equal sections. Six membrane panels could be inserted from alternate sides, supported on rectangular flange covers, and passed through vertical slits on the reactor wall. Consecutive membrane panels were separated by a vertical distance of 22 mm. There is a horizontal gap of 5 mm between the reactor wall and the unsupported end of the membrane panel. To evaluate the effects of the hydrogen withdrawal through the membranes, the reactor was also operated with no membrane panels, one membrane panel (fifth panel from the bottom), and six membrane panels, with dimensionally identical stainless steel dummy plates replacing the active membrane panels to keep the reactor internal geometry identical wherever the latter were not installed. The static bed height for all runs was 1.7 m.

The FBMR was operated under different operating conditions with a feed of steam mixed with methane, propane or heptane, with varying steam-to-carbon molar ratios. Experimental details are available elsewhere (5,6). The operating conditions for the runs compared with the simulations of this paper are given in Table 1.

The reactor was heated by internal cable heaters along the height of the dense catalyst bed at all four corners of the rectangular channel, in addition to external band heaters in the semi-circular spaces between the successive side openings for inserting and supporting membrane panels. The small scale of the reactor, and heat losses, especially close to the flanges, made the temperature profiles strongly dependent on the heater distribution.

Table 1: Experimental conditions for steam reforming of propane

Feed	Propane, Steam
Steam-to-carbon molar ratio	5.0
Average temperature	500°C
Reactor pressure	600 kPa abs
Permeate pressure	25 kPa abs
Total feed rate	0.614 mols/min

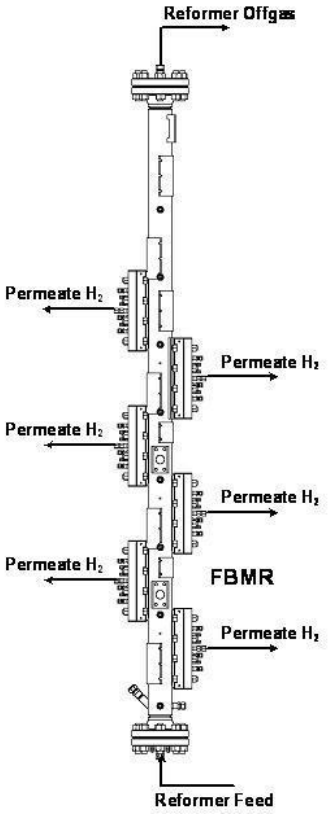

Figure 1: Fluidized bed membrane reactor showing six membranes for removal of pure hydrogen.

Commercial naphtha steam reforming catalyst particles, RK-212, of mean diameter from Haldor Topsoe A/S were crushed and sieved to a mean diameter of 179 μm.

REACTOR MODEL

The FBMR was modeled as two phases in parallel: a high-density dense phase, containing most of the particles, and a low-density bubble phase including a small number of particles, with the solids volume fraction assumed to be:

$$\phi_b = 0.001\varepsilon_b \tag{6}$$

The minimum fluidization velocity was estimated from the correlation of Grace (7). Model assumptions are:

(1) Steady state conditions.
(2) Ideal gas law.
(3) Catalyst temperature equal to local gas temperature. The axial variation in temperature is the same in each phase and follows the measured profile.
(4) Catalyst internal mass transfer resistance ignored.
(5) The membranes are infinitely selective, i.e. only H_2 passes through them.
(6) Catalyst deactivation is neglected.
(7) The gas in both the dense and bubble phases are assumed to be in plug flow.
(8) Visible bubble flow = flow in excess of that at minimum fluidization.

For each phase, the mole balance equation has four components:

(a) Reaction terms: The reactions are given by equations (1) ï (4), with rate equations as listed in an earlier paper (8).

(b) Interphase diffusional mass transfer: The interphase mass transfer coefficient is estimated by the correlation of Sit & Grace (9), with the effective diffusivity of gas components based on the average composition of the bubble and the dense phases, using the correlation of Wilke (10). The bubble size is estimated based on Dartonôs equation (11).

(c) Hydrogen permeation: The immersed membrane panels withdraw hydrogen from both phases, with the hydrogen flux governed by Sievertsôequation (12):

$$Q_{H_2,\varphi} = A_P \frac{P_{M0}}{\delta_{H_2}} \exp\left(\frac{-E_{H_2}}{RT}\right)\left(\sqrt{P_{H_2,\varphi}} - \sqrt{P_{H_2,m}}\right) \tag{7}$$

(d) Interphase convection to maintain with the two-phase theory of fluidization. For this, at a given height, the flow required in the dense phase is written as:

$$Q_{d,req} = U_{mf} A(1-\varepsilon_b) \tag{8}$$

Hence, the volumetric bulk convective terms can be written as:

when $\frac{R.T}{P}\sum_{i=1}^{N_C} F_{i,d} > Q_{d,req}$, $Q_{d\to b} = \frac{R.T}{P}\sum_{i=1}^{N_C} F_{i,d} - Q_{d,req}$, $Q_{b\to d} = 0$ (9)

when $\frac{R.T}{P}\sum_{i=1}^{N_C} F_{i,d} \le Q_{d,req}$, $Q_{b\to d} = Q_{d,req} - \frac{R.T}{P}\sum_{i=1}^{N_C} F_{i,d}$, $Q_{d\to b} = 0$ (10)

This way of maintaining the flow in the dense phase is consistent with CFD predictions for small particles (13).

Thus, the mole balance equation for the separation side can be written as:

$$\frac{dF_{H2,p}}{dL} = \alpha\left(\varepsilon_b Q_{mH_2,b} + (1-\varepsilon_b) Q_{mH_2,d}\right) \tag{11}$$

where α, (Ò1), the overall permeation effectiveness factor, is an adjustable parameter to fit the simulated hydrogen permeation yields to the experimental results.

For the i^{th} species in Bubble Phase:

$$\frac{dF_{i,b}}{dh} = \phi_b \rho_p A \sum_{j=1}^{N_R} \gamma_{ij} R_{j,b} + k_{iq} a_b \varepsilon_b A\left(C_{i,d} - C_{i,b}\right) - \alpha \varepsilon_b Q_{m\,i,b} - \frac{dQ_{bd}}{dh} C_{i,b} + \frac{dQ_{db}}{dh} C_{i,d}$$

with i = C_7H_{16}, C_3H_8, CH_4, H_2O, CO, CO_2, and H_2 (12)

A similar mole balance is written for the i^{th} species in the dense phase. The flux of all components other than hydrogen through the membranes is zero.

To predict the reactor offgas composition, it is also necessary to account for catalytic reaction in the freeboard. An amount of catalyst equivalent to 0.8 mm of static bed depth was assumed to be distributed uniformly in the freeboard region, based on least squares error minimization with respect to the experimental concentrations of methane, CO_2, and H_2 in the reformer off-gas for all of the experimental runs. The freeboard was then modeled as a single-phase dilute suspension, with

$$\frac{dF_{i,fb}}{dh_{fb}} = \phi_{fb} \rho_p A \sum_{j=1}^{NR} \gamma_{ij} R_{j,fb} \tag{13}$$

The following quantities are calculated to assess the reactor performance:

$$\text{Permeate hydrogen yield} = \frac{\text{molar flow of pure } H_2 \text{ extracted via membranes}}{\text{molar flow of hydrocarbon in feed stream}} \tag{14}$$

$$\text{Total hydrogen yield} = \frac{\text{molar flow of pure } H_2 \text{ extracted via membranes} + \text{molar flow of } H_2 \text{ in retentate stream}}{\text{molar flow of hydrocarbon in feed stream}} \tag{15}$$

$$\text{Carbon oxides yield} = \frac{\text{total molar flow of CO and } CO_2 \text{ in retentate stream}}{\text{molar flow of carbon (in hydrocarbon) in feed stream}} \tag{16}$$

$$\text{Methane yield} = \frac{\text{molar flow of methane in retentate stream}}{\text{molar flow of carbon (in hydrocarbon) in feed stream}} \tag{17}$$

RESULTS AND DISCUSSION

Temperature profiles for the experiments, greatly affected by the heater arrangement, are shown in each plot below. The model was used (8) to simulate previous experimental results (5,6), and good agreement was achieved with α as the only adjustable parameter. Fitting of experimental data to the model for hydrogen permeation through the membranes gave α = 0.248 as a correction to a membrane permeation equation provided by the suppliers of the membrane panels. The decline in permeation flux relative to that in tests in a permeation test rig without particles was likely due to formation of a thin coating of catalyst fines on the membrane foils.

Figure 2 plots the superficial gas velocities for propane steam reforming with six membrane panels. Four factors caused the variations in superficial velocity:

(1) Intermittent abrupt variations of the superficial gas velocity due to changes in cross-sectional area in the spaces between adjacent membrane panels.
(2) The superficial gas velocity is affected by the temperature variations.
(3) The steam reforming reactions lead to a net increase in molar flow. This caused steep increases in U near the FBMR entrance, where propane conversion is completed. Subsequent methanation (reverse reactions from equations (2) and (4)) can result in the opposite trend.

(4) Superficial velocity also varies owing to hydrogen removal via the membranes.

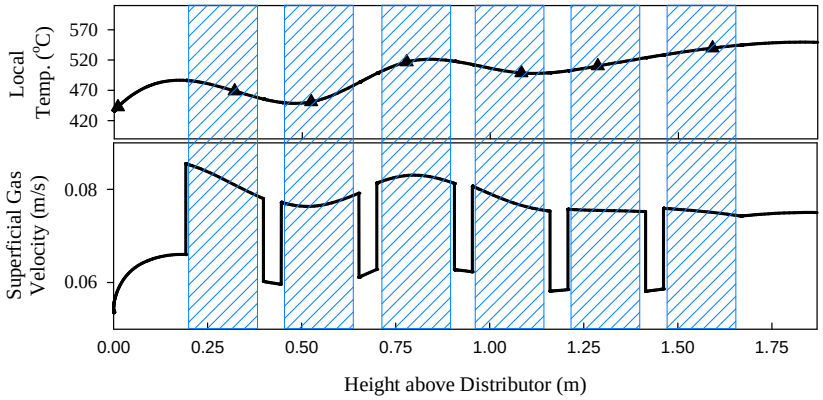

Figure 2: Gas superficial velocities for propane steam reforming.

The sensitivity of the reactor model was tested (8) to understand the relative importance of the various phenomena inside the FBMR, as well as the effect of uncertainties in estimating parameters in the model. The bulk mass transfer was found to be negligible compared to the other three components of the mole balance equations. Similar observations apply to steam methane reforming in an FBMR (14).

The kinetic rate constants for all reactions included were first varied upwards and downwards by a factor of 10 compared with those based on the literature values. Some variations in performance occurred near the reactor entrance, affected mainly by the propane steam reforming kinetics. However, over most of the height, there was very little difference in the local yields of methane, carbon oxides or hydrogen.

To test the importance of hydrodynamics and interphase mass transfer, Figure 3 shows the reactor performance with the interphase mass transfer coefficient increased and decreased a factor of 10 relative to those from the Sit and Grace (9) correlation. The higher coefficient results in almost immediate transfer of propane from the bubbles to the dense phase, whereas, slower mass transfer retains more propane in the bubbles, delaying its conversion, Since methane is an intermediate component, it appears more slowly in the reactor, and its overall conversion is also delayed. With delayed transfer of hydrogen from the dense phase, where it is produced, to the bubble phase, where negligible hydrogen is produced, the net removal of hydrogen via membranes is reduced.

While the effects of tenfold upward and downward changes in the interphase mass transfer coefficient are discernible, these effects are not very significant. Hence, interphase mass transfer, while not a negligible factor, plays a secondary role with respect to overall reaction. Since the bed hydrodynamics mostly enter the model through the interphase mass transfer, one may also conclude that accurate portrayal of bed hydrodynamics is of secondary importance for this process and for the operating conditions investigated.

To explore the effect of permeation capacity variation of the membranes, the membrane permeation effectiveness factor was set at α = 0.15, 0.248 (fitted value), and 0.35. As shown by Figure 4, the FBMR performance depends strongly on the hydrogen permeation through the membranes.

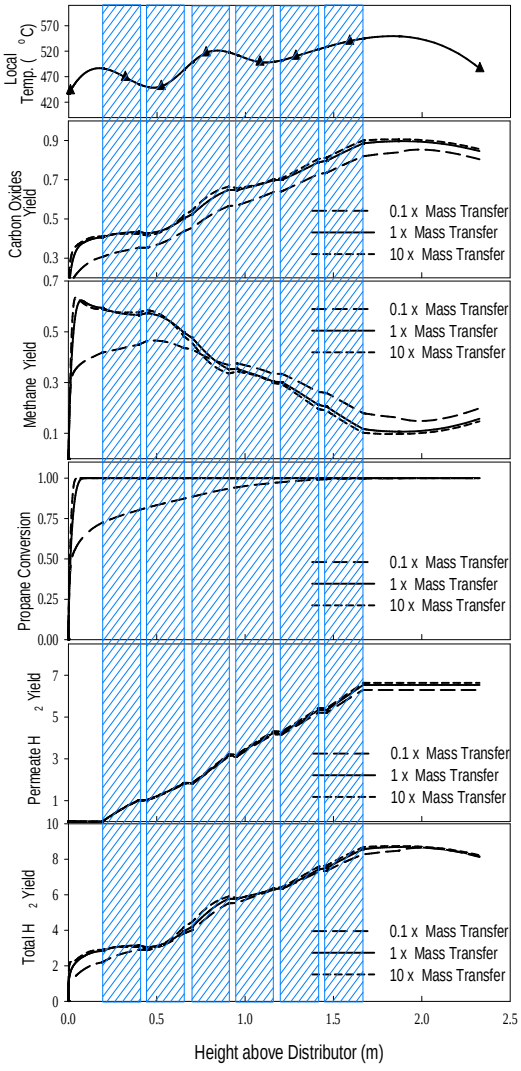

Figure 3: FBMR performance with variations in interphase mass transfer coefficient

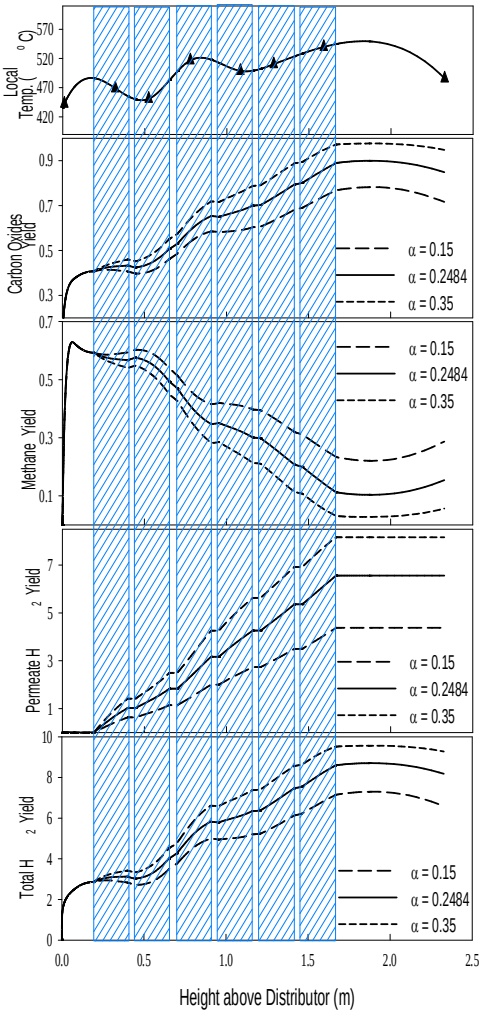

Figure 4: FBMR performance with variations in permeation effectiveness factor.

CONCLUSIONS

A fluidized bed membrane reactor is modeled to simulate its performance for producing hydrogen from propane. Model sensitivity studies show that the chemical kinetics are fast enough at all temperatures tested for their role to be insignificant in determining the FBMR performance. The interphase diffusional mass transfer rate is somewhat more significant in affecting reactor performance, but again plays a secondary role. From these results, it is evident that the FBMR performance is primarily controlled by chemical equilibrium and by the rate of hydrogen permeation through the membranes. Hence the model is sensitive to accurately characterizing

the chemical equilibrium and hydrogen permeation, but insensitive to the chemical kinetics, interphase mass transfer and hydrodynamics, at least for the temperature range of interest (450-550°C).

ACKNOWLEDGEMENT

Financial support from the Canada Foundation for Innovation and the Natural Sciences and Engineering Research Council of Canada (NSERC) is gratefully acknowledged. M.A.R. thanks NSERC for a two-year doctoral scholarship.

NOTATION

a_b	Specific surface area of gas bubbles (m^2/m^3)
A	Cross-sectional area of bed (m^2)
A_P	Membrane permeation area per unit length of membrane (m^2/m)
$C_{i,b}$	Molar concentration of species *i* in bubble phase (mol/m^3)
$C_{i,d}$	Molar concentration of species *i* in dense phase (mol/m^3)
E_{H_2}	Activation energy for permeation (J/mol)
$F_{i,b}$	Molar flow rate of species *i* in bubble phase (mol/s)
$F_{i,d}$	Molar flow rate of species *i* in dense phase (mol/s)
$F_{i,fb}$	Molar flow rate of species *i* in freeboard (mol/s)
h	Vertical coordinate measured from distributor (m)
h_{fb}	Vertical co-ordinate from dense catalyst bed surface (m)
k_{iq}	Interphase mass transfer component for species *i* (m/s)
m, n	Stoichiometric constants (-)
N_C, N_R	Number of components, reactions (-)
P	Pressure (Pa)
P_i	Partial pressure of species *i* (bar)
$P_{H_2,b}$, $P_{H_2,d}$	Partial pressure of hydrogen in bubble, dense phase (atm)
$P_{H_2,p}$	Partial pressure of hydrogen on permeate side (atm)
P_{M0}	Pre-exponential factor for permeation ($mole/(m.min.atm^{0.5})$)
Q_{bd}	Cross-flow from bubble to dense phase per unit length ($m^3/(m.s)$)
Q_{db}	Cross-flow from dense to bubble phase per unit length ($m^3/(m.s)$)
$Q_{d,req}$	Flow requirement for dense phase to prevent de-fluidization (m^3/s)
$Q_{mi,\varphi}$	Membrane permeation rate of species *i* for φ phase ($mol/(m.s)$)
R	Universal gas constant (J/mol/K)
R_j	Rate of j^{th} reaction (mol/kg catalyst/s)
U	Superficial gas velocity (m/s)
δ_{H_2}	Thickness of hydrogen selective membranes (m)
ε_b	Volume fraction of catalyst bed occupied by bubble phase (-)
ϕ_b, ϕ_d	Bed volume fraction occupied by particles in bubble, dense phase (-)
ϕ_{fb}	Volume fraction of freeboard occupied by solid particles (-)

γ_{ij}	Stoichiometric coefficient of component *i* in j^{th} reaction
ρ_p	Density of catalyst particles (kg/m^3)
ΔH	Heat of reaction (kJ/mol)

Subscripts

b, d	Bubble, dense phase
fb	Freeboard
i	Species *i*
in	At reactor inlet
j	Reaction *j*
m	Membrane side
φ	Phase φ

REFERENCES

1. Rostrup-Nielsen, J., Catalytic steam reforming. In *Catalysis Science and Technology*, Andersen, J.R.; Boudart, M., Eds. Springer-Verlag: 1984; pp 1-117
2. Adris, A.M.; Lim, C.J.; Grace, J.R., The fluidized bed membrane reactor system: A pilot scale experimental study. *Chem. Eng. Sci.* 1994, 49, 5833-5843.
3. Boyd, T.; Grace, J.; Lim, C.J.; Adris, A.M., Hydrogen from an internally circulating fluidized bed membrane reactor. *Int. J. Chem. React. Eng.* 2005, 3, A58.
4. Patil, C.S.; Annaland, M.V.S.; Kuipers, J.A.M., Fluidised bed membrane reactor for ultrapure hydrogen production via methane steam reforming: Experimental demonstration and model validation. *Chem. Eng. Sci.* 2007, 62, 2989-3007.
5. Rakib, M.A.; Grace, J.R.; Lim, C.J.; Elnashaie, S.S.E.H., Steam reforming of heptane in a fluidized bed membrane reactor. *J. Power Sources* 2010, 195, 5749-5760.
6. Rakib, M.A.; Grace, J.R.; Lim, C.J.; Elnashaie, S.S.E.H.; Ghiasi, B., Steam reforming of propane in a fluidized bed membrane reactor for hydrogen production. *Int. J. Hydrogen Energy* 2010, 35, 6276-6290.
7. Grace, J.R., Fluidized-bed hydrodynamics. In *Handbook of Multiphase Systems*, Hetsroni, G., Ed. Hemisphere: Washington, 1982; pp 8-5 - 8-64.
8. Rakib, M.A.; Grace, J.R.; Lim, C.J.; Elnashaie, S.S.E.H., Modeling of a fluidized bed membrane reactor for hydrogen production by steam reforming of hydrocarbons. *Ind. Eng. Chem. Res.*, 2011, In Press.
9. Sit, S.P.; Grace, J.R., Effect of bubble interaction on interphase mass transfer in gas fluidized beds. *Chem. Eng. Sci.* 1981, 36, 327-335.
10. Wilke, C. R., Diffusion properties of multicomponent gases. *Chem. Eng. Prog.* 1950, 46, 95-104.
11. Darton, R.C.; Lanauze, R.D.; Davidson, J.F.; Harrison, D., Bubble growth due to coalescence in fluidized-beds. *Trans. IChemE* 1977, 55, 274-280.
12. Sieverts, A.; Zapf, G., The solubility of deuterium and hydrogen in solid palladium. *Zeitschrift für Physikalische Chemie* 1935, 174, 359-364.
13. Li, T.W.; Mahecha-Botero, A.; Grace, J.R., Computational fluid dynamic investigation of change of volumetric flow in fluidized bed reactors. *Ind. Eng. Chem. Res.* 2010, 49, 6780-6789.
14. Adris, A.M.; Lim, C.J.; Grace, J.R., The fluidized-bed membrane reactor for steam methane reforming: Model verification and parametric study. *Chem. Eng. Sci.* 1997, 52, 1609-1622.